AIAA JOURNAL
Vol. 41, No. 7, July 2003

Control of Supersonic Impinging Jet Flows Using Supersonic Microjets

F. S. Alvi,* C. Shih,† R. Elavarasan,‡ G. Garg,§ and A. Krothapalli¶
Florida A&M University and Florida State University, Tallahassee, Florida 32310

Supersonic impinging jets, such as those occurring in the next generation of short takeoff and vertical landing aircraft, generate a highly oscillatory flow with very high unsteady loads on the nearby aircraft structures and the landing surfaces. These high-pressure and acoustic loads are also accompanied by a dramatic loss in lift during hover. Previous studies of supersonic impinging jets suggest that the highly unsteady behavior of the impinging jets is due to a feedback loop between the fluid and acoustic fields, which leads to these adverse effects. A unique active control technique was attempted with the aim of disrupting the feedback loop, diminishing the flow unsteadiness, and ultimately reducing the adverse effects of this flow. Flow control was implemented by placing a circular array of 400-μm-diam supersonic microjets around the periphery of the main jet. This control approach was very successful in disrupting the feedback loop in that the activation of the microjets led to dramatic reductions in the lift loss (40%), unsteady pressure loads (11 dB), and near-field noise (8 dB). This relatively simple and highly effective control technique makes it a suitable candidate for implementation in practical aircraft systems.

I. Introduction

AN UNDERSTANDING of the impinging jet flowfield is necessary for the design of efficient short takeoff and vertical landing (STOVL) aircraft. When such STOVL aircraft are operating in hover mode, that is, in close proximity to the ground, the downward-pointing lift jets produce high-speed, hot flow that impinges on the landing surface and generates the direct lift force. It is well known that in this configuration several flow-induced effects can emerge, which substantially diminish the performance of the aircraft. In particular, a significant lift loss can be induced due to flow entrainment by the lifting jets from the ambient environment in the vicinity of the airframe. Other adverse phenomena include severe ground erosion on the landing surface and hot gas ingestion into the engine inlets. In addition, the impinging flowfield usually generates significantly higher noise levels relative to that of a freejet operating under similar conditions. Increased overall sound pressure levels (OASPL) associated with the high-speed impinging jets can pose an environment pollution problem and adversely affect the integrity of structural elements in the vicinity of the nozzle exhaust due to acoustic loading. Moreover, the noise and the highly unsteady pressure field are frequently dominated by high-amplitude discrete tones, which may match the resonant frequencies of the aircraft panels, thus further exacerbating the sonic fatigue problem.

These problems become more pronounced when the impinging jets are supersonic, the operating regime of the STOVL version of the future joint strike fighter. In addition, the presence of multiple impinging jets can potentially further aggravate these effects due to the strong coupling between the jets and the emergence of an upward-moving fountain flow flowing opposite to the lift jets.[1] A schematic of a generic STOVL aircraft with multiple lift/impinging jets is shown in Fig. 1, where various regions where these problems might occur have been indicated.

Received 7 August 2000; revision received 14 February 2003; accepted for publication 3 March 2003.

*Associate Professor, Department of Mechanical Engineering, 2525 Pottsdamer Street. Senior Member AIAA.
†Professor, Chairman, Department of Mechanical Engineering, 2525 Pottsdamer Street. Associate Fellow AIAA.
‡Postdoctoral Research Associate, Department of Mechanical Engineering, 2525 Pottsdamer Street. Member AIAA.
§Graduate Research Assistant, Department of Mechanical Engineering, 2525 Pottsdamer Street. Student Member AIAA.
¶Don Fuqua Eminent Professor, Department of Mechanical Engineering, 2525 Pottsdamer Street. Associate Fellow AIAA.

A. Feedback Loop

To minimize their adverse influence on aircraft performance, it is evident that the undesirable effects of supersonic impinging jets need to be controlled. However, before one can devise an effective control scheme to eliminate these detrimental characteristics, one must have a fundamental understanding of the principal physical mechanisms governing these flows. The acoustic properties of single supersonic impinging jet flowfield have been investigated by a number of researchers, including Powell,[2] Neuwerth,[3] and Tam and Ahuja.[4] These studies conclusively demonstrated that the unsteady properties of impinging jet flows are dominated by the presence of discrete impingement tones. These high-amplitude tones are generated by highly coherent instability waves due to the emergence of a self-sustained feedback loop. For a detailed discussion of the feedback mechanism, see Refs. 2–4. Very briefly, large-scale vortical structures in the jet shear layer impinge on the wall and generate coherent pressure fluctuations, which result in acoustic waves of significant intensity. These acoustic waves travel through the ambient medium and, on reaching the nozzle (a region of high receptivity), excite the shear layer of the jet. This leads to the generation of a new set of enhanced instability waves, which rapidly evolve into large-scale vortical structures, thus closing the feedback loop. A similar feedback mechanism is also responsible for the production of discrete tones such as screech tones, which are conspicuously present in nonideally expanded, that is, over- or underexpanded, and edge tones generated due to the presence of an "edge" in the jet hydrodynamic field . In fact, the feedback mechanism responsible for discrete tones was first clearly articulated by Powell in classic papers on jet noise[5] and on the feedback loop responsible for edge tones.[6]

Flow properties of high-speed impinging jets have also been examined by a number of investigators, including Donaldson and Snedeker,[7] Carling and Hunt,[8] and Lamont and Hunt,[9] among others. These studies mainly emphasized the mean properties of this flow with most of the measurements limited to mean surface properties, such as the pressure distributions on the impingement surface. Recently, Krothapalli et al.[10] conducted an extensive investigation to obtain a better understanding of the physics governing some of the mean and unsteady properties of such flows, using the geometry shown in Fig. 2. One of the main findings of their work was the intimate connection between the discrete impinging tones and the

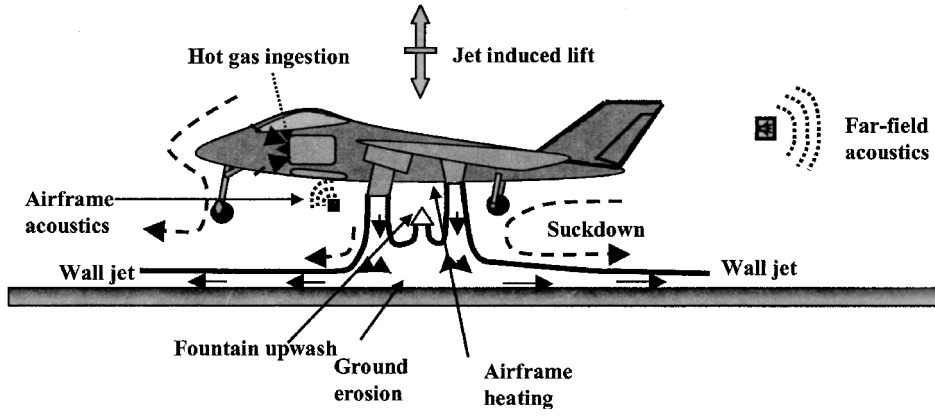

Fig. 1 Flowfield created by the propulsion system around a STOVL aircraft.

highly unsteady, oscillatory behavior of the impinging jet column. They demonstrated that, through the generation of large-scale structures in the jet shear layer, the feedback phenomenon might also be responsible for lift loss on the surfaces in the vicinity of the nozzle. These structures induce higher entrainment velocities that lead to lower pressures on surfaces in the jet vicinity and, consequently, a significant loss in lift.

In a companion study, Alvi and Iyer[11] noted the emergence of discrete peaks in the spectra of the unsteady surface pressures, which match the impinging tone frequencies in the near-field acoustic measurements. This suggests that these feedback loop-driven flow instabilities are also responsible for the unsteady loads on the ground plane. In some cases these measured unsteady loads were extremely high, as high as 190 dB. When coupled with the high temperatures associated with lifting jets, such high loads can severely aggravate the ground erosion problem.

B. Control of the Feedback Loop: Prior Attempts

Based on the preceding discussion, it is apparent that, to eliminate effectively these unwanted effects of impinging jet flows, one must reduce the highly unsteady behavior of the impinging flow by weakening the feedback loop. There are various potential approaches for disrupting the feedback loop and achieving a measure of control of the unsteady properties of this flow. For example, one could 1) intercept the upstream propagating acoustic waves so that they can not complete the feedback loop, and/or 2) manipulate the shear layer (for example, increase its thickness) near the nozzle lip, hence reducing its receptivity to the acoustic disturbances, and/or 3) disrupt the coherent interaction between the flow instabilities and the acoustic field by tickling the nozzle shear layer using a disturbance at or very near the nozzle exit. The source of these disturbances could in principal be passive, such as those generated by tabs at the nozzle exit, or they could be active in nature, such as the use of high-energy acoustic and/or fluidic sources near the nozzle exit.

Based on these concepts, a number of attempts have been made in the past to suppress the feedback mechanism. For instance, Karamcheti et al.[12] successfully suppressed edge tones in low-speed flows, which are governed by a similar feedback mechanism, by placing two plates normal to the centerline of the jet. Motivated by their work, Elavarasan et al.[13,14] employed a similar technique to attenuate the feedback loop in an impinging jet flow by introducing a control plate near the nozzle exit. Using this approach, they were able to intercept the upstream propagating acoustic waves, thus disrupting the feedback loop. As anticipated, attenuation of the loop led to a measurable weakening of the large-scale structures in the jet flow. For selected cases, this passive control approach resulted in a maximum recovery of about 16% of the lift loss relative to an uncontrolled impinging jet. Similarly for a few cases, Elavarasan et al.[13,14] also reported a reduction of about 6–7 dB in the near-field OASPL. Glass[15] and Poldervaart et al.[16] used similar passive control techniques with limited success. In a series of experiments reported

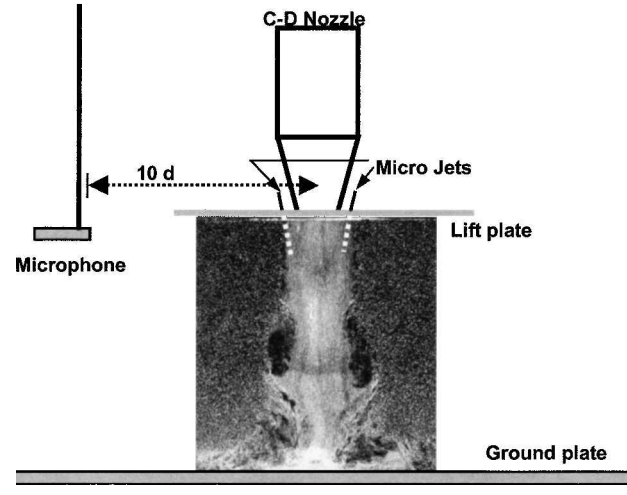

Fig. 2 Schematic of the experimental arrangement.

by Samimy et al.[17] and Zaman et al.,[18] the effect of passive tabs on the aeroacoustic properties of supersonic jets was also investigated. Although the tabs were able to attenuate the screech tones, significant reduction in the OASPL was achieved by using multiple tabs,[17] which also resulted in significant thrust loss, as high as 12% (Ref. 18).

Consequently, although passive control techniques have been able to weaken the feedback mechanism, gains are usually accompanied by a significant cost, such as thrust loss.[17,18] In addition, any significant performance gains are confined to a limited range of operating conditions, especially for impinging jets. This is because relatively small changes in the nozzle-to-ground separation h/d can lead to significant changes in the magnitude and frequency of the tones responsible for the flow unsteadiness,[11] changes to which passive techniques cannot readily respond. Consequently, any efficient control technique aimed at suppressing the feedback loop must be active and capable of adapting to the shift in frequencies/wavelengths of the modes that lock on to the feedback loop.

In a recent study, Sheplak and Spina[19] used high-speed coflow to shield the main jet from the near-field acoustic disturbances. For a suitable ratio of the main jet and coflow exit velocity, they measured a reduction of greater than 10 dB in the near-field broadband noise level. In addition to noise reduction, the impinging tones were also significantly suppressed using this approach. Although effective, the high mass flow rates of the coflowing jet required to achieve this noise reduction, around 20–25% of the main jet mass flux, limit the practical applicability of this coflow approach. Shih et al.[20] used a counterflowing stream near the nozzle exit to suppress successfully screech tones of nonideally expanded jets. They were also able to obtain modest reductions in OASPL, approximately 3–4 dB, while

enhancing the mixing of the primary jet. However, these active control schemes require additional design modifications and/or high operating power, rendering them often impractical for implementation in aircraft.

C. Present Approach for Flow Control

In the current program, we are proposing the implementation of a control-on-demand strategy using microactuators in the form of supersonic microjets. These microjets are extremely small and require very low mass flux. Although further details of these microjets are discussed later, note that one of the most significant advantages of using microactuators is that their extremely small size allows these systems to be operated in places where traditional systems cannot work due to either space limitation or a lack of system response.

In principal, by populating the appropriate region on the lift plate, in the vicinity of the nozzle exit for the present case, one could develop a system where the most appropriate microjets would be strategically turned on and off to provide optimal control. The proposed control system would have the advantage that, depending on the operating and local flow conditions, optimal flow control can be achieved by activating the pertinent supersonic microjets with the appropriate magnitude and frequency (if possible) and at the desired time. In contrast to the traditional passive control methods, the proposed control-on-demand system can be switched on and off strategically. We are presently in the initial stages of implementing the adaptive portion of this technique, that is, the ability to selectively activate appropriate microjets. Although still preliminary in nature, the results demonstrate considerable promise for implementing adaptive flow control using microjets. See Lou et al.[21] for these results. Such a system should not measurably influence the operational performance of the aircraft when it is not needed. The very small size of the hardware and the minimal mass flow rates require minimal power consumption and is expected to result in negligible, if any, thrust loss of the primary jet.

In the present experiments, microjets were made using 400-μm-diam stainless tubes, and 16 supersonic microjets were distributed around the nozzle exit (Fig. 3a). Based on the earlier discussion of the feedback loop, it is evident that the presence of these supersonic microflow streams can be effective in weakening the loop in a number of ways. First, the microjet streams may play a role in the interception of the upstream propagating acoustic disturbances. Second, these high-momentum jets can provide spatial/temporal distortions to the coherent shear layer instabilities, thus disrupting their interactions with the acoustic field. A more detailed description of the microjet hardware is provided in Sec. II, the experimental methods section.

Finally, note that the purpose of this study is not to perform a systematic, exhaustive investigation of the microjet system necessary to achieve optimal control over a large parametric space. Rather, in this proof-of-concept study, our aim is to examine the feasibility and potential benefits of using microjets to alleviate the adverse effects of the supersonic impinging jet flowfield. The influence of this control strategy on the flow behavior was studied using flow visualization, microphone measurements, and mean and unsteady surface pressure measurements. As the results presented in this paper illustrate, there is convincing evidence that the proposed control strategy is very promising as a means of effectively controlling supersonic impinging jet flowfields.

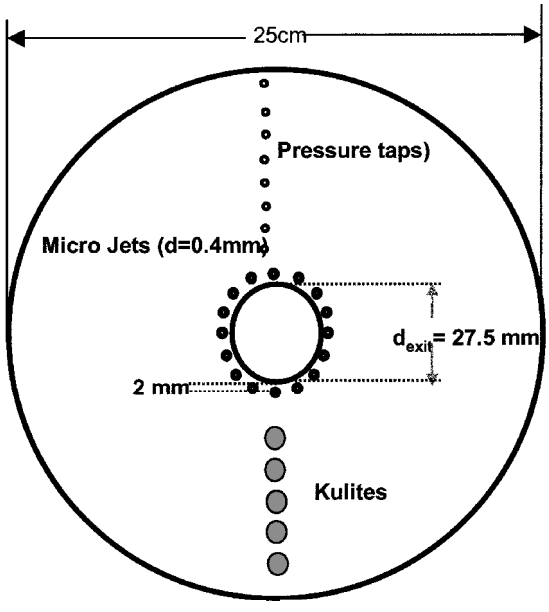

Fig. 3a Geometry of the lift plate and microjets.

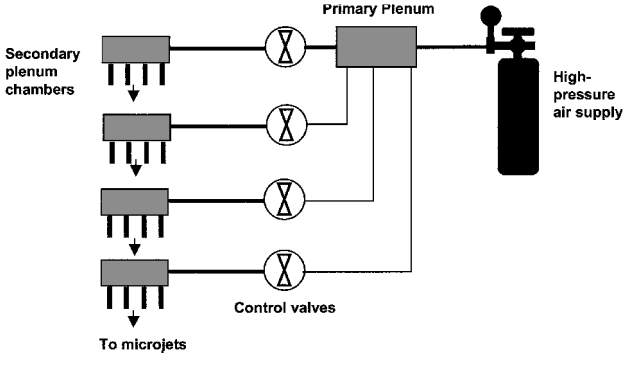

Fig. 3b Microjets supply assembly.

II. Experimental Hardware and Techniques

The experiments were carried out at the STOVL supersonic jet facility of the Fluid Mechanics Research Laboratory located at the Florida State University. A schematic of the facility with a single impinging jet is shown in Fig. 2. This facility is used primarily to study jet-induced phenomenon on STOVL aircraft hovering in and out of ground effect. Facility details can be found by Wardwell[22] and Krothapalli et al.[10]; only a very brief description is provided here.

The measurements were carried using a shock-free, nearly ideally expanded jet issuing from a convergent–divergent (C–D) axisymmetric nozzle. The throat and exit diameters $\boldsymbol{d}$ and $\boldsymbol{d}_e$ of the nozzle are 2.54 and 2.75 cm, respectively. The divergent part of the nozzle is a straight-walled conic section with a 3-deg divergence angle from the throat to the nozzle exit. The nozzle was designed for an exit Mach number of 1.5 and operated at a nozzle pressure ratio [(NPR) where NPR is the ratio of stagnation pressure/ambient pressure] of 3.7 to produce a nominally, ideally expanded impinging jet. The primary reason for running an ideally expanded jet was to isolate the effect of the impingement tones from screech tones because the latter only occur in jets operating at off-design conditions. A circular plate of diameter 25.4 cm ($\sim 10\boldsymbol{d}$) was flush mounted with the nozzle exit. The circular plate, henceforth referred to as the lift plate, represents a generic aircraft planform and has a central hole, equal to the nozzle exit diameter, through which the jet is issued. A 1 m $\times$ 1 m $\times$ 25 mm aluminum plate serves as the ground plane; it is mounted directly under the nozzle on a hydraulic lift (Fig. 2).

The flow-induced lift forces were estimated by measuring the mean pressure distribution on the lift plate. This was accomplished by using an array of pressure taps arranged along a radial line on the lift plate. The pressure measurements were obtained by scanning the static pressure ports using a Scanivalve™ system connected to a Validyne™ strain gauge transducer. In addition, high-frequency response miniature Kulite™ pressure transducers were also mounted on the lift plate along a radial line, as shown in Fig. 3a, and were used to measure the unsteady pressure loads on the lift plate. The lift plate data shown in this paper are obtained from a single Kulite located approximately 35 mm from the nozzle lip. The unsteady pressure field created by the jet impingement on the ground plane was measured with two additional high-frequency 100-psi (6.9×10^5 Pa) Kulite pressure

transducers (Model XCQ-062-100), one at the impingement point on the jet centerline and the other 25 mm away from the centerline. The near-field acoustic measurements were made using a 0.635-cm-diam B&K microphone placed 25 cm away from the nozzle exit oriented 90 deg to the jet axis. To minimize sound reflections during the near-field acoustic measurements, near by exposed metal surfaces were covered with thick acoustic foam. The flow was visualized using a conventional, single-pass shadowgraph arrangement where a stroboscopic white-light flash unit with variable pulse frequency of up to 1 kHz was used as a light source.

The microphone and the lift plate surface pressure signals were acquired through National Instruments digital data acquisition cards using LabView™ software. For unsteady measurements, that is, microphone and Kulite data, 102,400 points were recorded for each signal. Standard statistical analysis techniques were used to obtain the spectral content and the OASPL from these measurements. The spectral content of the unsteady signals was obtained by segmenting each data record into 100 subgroups with 1024 points each, and a fast Fourier transform (FFT) with a frequency resolution of 68.4 Hz was computed for each segment. The 100 FFTs thus obtained were averaged to obtain a statistically reliable estimate of the narrow-band noise spectra. The estimated uncertainty associated with the unsteady lift plate pressure P_{rms} is ± 0.02 psi, whereas the rms intensities of the ground plane pressures were estimated to be accurate within ± 0.2 psi. Note that when the unsteady pressures are expressed in decibels, a fixed error in pounds per square inch translates into different errors in decibels, depending on the overall value of P_{rms}. The P_{rms} values on the lift plate are around 160 dB (shown subsequently) for the cases of interest, which results in an uncertainty of approximately 0.6 dB. Similarly, the dynamic pressure levels on the ground plane are in the range of 180 dB, which also translates into an uncertainty of approximately 0.6 dB. The microphone signal was measured with an estimated uncertainty of ± 1 dB.

The main controlling parameter in the experiment was the ground plate height h with respect to the nozzle exit, which was varied from $2\boldsymbol{d}$ to $60\boldsymbol{d}$. As stated earlier, the experiments discussed here were conducted at NPR = 3.7, which corresponds to a nearly ideally expanded primary jet flow. The jet stagnation temperature was maintained at $20 \pm 2^{\circ}$C. The nominal exit Reynolds number at exit of the nozzle was 7×10^5 (based on exit velocity and nozzle diameter).

Active flow control was implemented using 16 microjets, flush mounted circumferentially around the main jet as shown in the Fig. 3a. The jets were produced using 400-μm-diam stainless tubes, mounted on the lift plate with an inclination of approximately 20 deg with respect to the primary jet axis. The supply for the microjets was provided from a compressed air cylinder through a main and four secondary plenum chambers (Fig. 3b). The high-pressure air was passed through a micrometer-sized filter to prevent the micronozzles from becoming clogged. The secondary plenum chambers ensured that the flow coming out of the microjets was relatively free of unsteadiness. The microjets were connected to the secondary plenum chamber through four solenoid-controlled valves in such a way that any four microjets can be controlled (on/off) individually. The microjets were operated at an NPR of approximately 7. At this operating condition, the combined mass flow rate of all 16 microjets was well below 0.5% of the primary jet mass flux.

III. Discussion of Results

A. Impinging Jet Without Control

Figure 4 shows instantaneous shadowgraph images of the impinging jet flowfield at $h/d = 4.5$ with and without control, whereas Fig. 5 shows phase-averaged images under the same conditions. (Note that all linear dimensions in this paper are nondimensionalized by the nozzle throat diameter $\boldsymbol{d}$.) Although both cases, with and without control, are shown here, a discussion of the effect of control is delayed until the next subsection. The instantaneous shadowgraph for the uncontrolled case, that is, microjets off, in Fig. 4a clearly shows the presence of multiple, strong, acoustic waves. These waves signify the presence of impinging tones, and as seen in the image, they impinge and reflect from nearby surfaces, represented by the

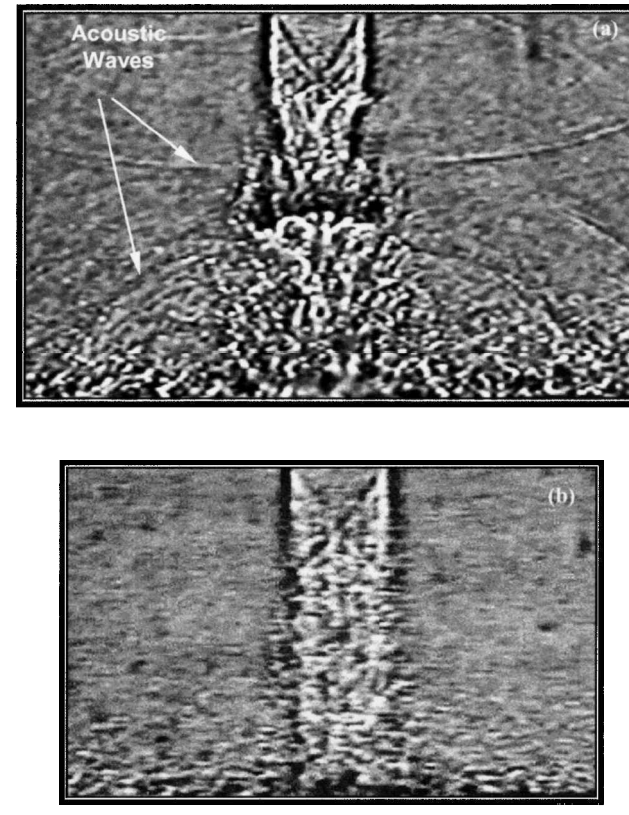

Fig. 4 Instantaneous shadowgraph images, NPR = 3.7 and $h/d = 4.5$: a) no control and b) with microjet control.

lift plate in the present case. Concomitant with the appearance of the acoustic waves is the emergence of large-scale structures in the jet shear layer. Such structures can be clearly seen in both the instantaneous and phase-averaged shadowgraphs in Figs. 4a and 5a, where they have also been marked for clarity. The phase-averaged image was obtained by triggering the light source at a subharmonic of the dominant impinging tone frequency such that 15–16 pulses are averaged per frame to produce the phase-averaged image. As discussed in the Introduction, such large-scale structures, not normally observed in high-speed jets, significantly increase jet entrainment velocities[10,13,14] leading to lift loss. Furthermore, the presence of such distinct, stationary structures in the phase-averaged images visually indicates that, in addition to the acoustic field, the unsteady flow properties are also dominated by periodic, discrete frequency disturbances, a fact confirmed by the quantitative measurements discussed next.

The spectral content of the unsteady fluid and acoustic properties is examined via the narrow-band spectra of the near-field microphone, unsteady lift plate, and ground plane pressures shown in Figs. 6 and 7 for $h/d = 3$ and 4.5 in., respectively. (In Figs. 6 and 7, as in all subsequent similar plots, the fluctuating pressures have been expressed in decibels, using a 20-μPa reference.) Although data for the ground plane are only shown for the Kulite transducer located on the impinging jet centerline, the behavior of the unsteady ground plane pressures at other transducer locations is very similar. One of the most significant features in both Figs. 6 and 7 is the presence of discrete, high-amplitude, multiple peaks that are indicative of impingement tones due to the feedback loop. An examination of the microphone and unsteady pressure data for a fixed height reveals that the resonant tones occur at identical frequencies for all three transducer locations. This supports our earlier observation based on the visual evidence in Fig. 5a and further confirms the global nature of the flow oscillations generated by the feedback loop. A comparison of spectra for $h/d = 3$ with $h/d = 4.5$ in Figs. 6 and 7, respectively, shows that the frequencies at which these tones occur change with nozzle height.

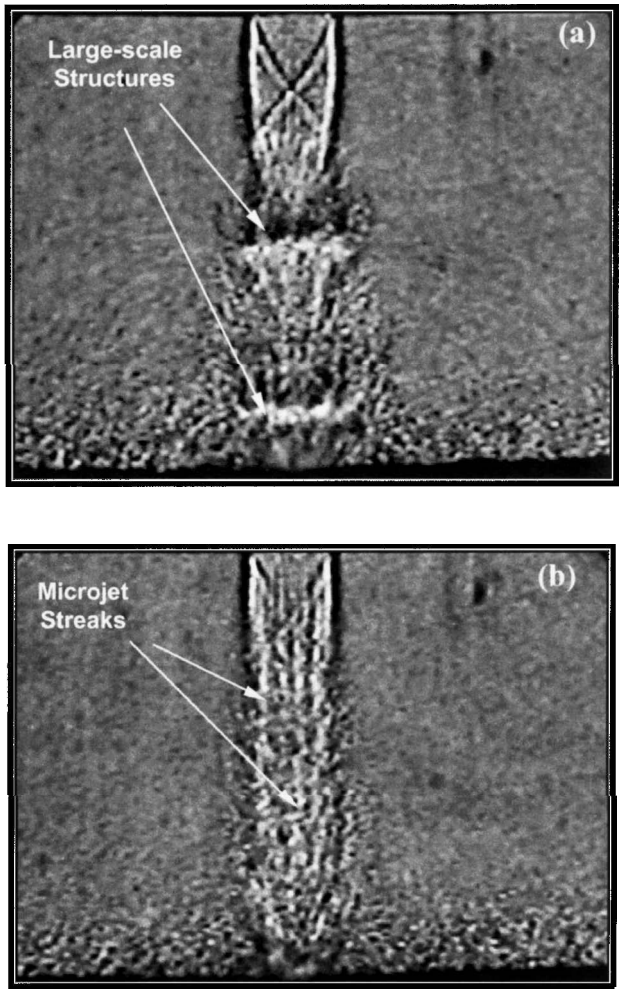

Fig. 5 Phase-averaged shadowgraph images, NPR = 3.7 and $h/d = 4.5$: a) no control and b) with microjet control

Although not shown here, a similar shift in frequencies is also observed with respect to NPR.[11] Furthermore, because the unsteady properties of this flowfield, as is the case for most flows governed by a feedback loop, are extremely sensitive to local boundary conditions, experiments conducted at the same facility, under the same nominal conditions,[21] can display some variations in the unsteady properties, such as a shift in the tone frequencies and amplitudes. The strong dependence of the unsteady flowfield on the operating conditions suggests that an efficient control technique must be able to adapt to such changes in the feedback loop for optimal control.

The intensities of the unsteady pressure fluctuations, P_{rms}, on the lift and ground planes as well as the near-field noise are shown in Fig. 8 as a function of the ground plane height. The rms pressure levels on the ground plane have the highest magnitude, in the 180–190-dB range (corresponding to $P_{\text{rms}} \approx$ 3–9 psi), which is to be expected because the primary jet flow directly impinges on the ground plane. Such high unsteady loads on the ground plane can cause significant ground erosion of the landing surface, especially when combined with the thermal loads generated by the impingement of hot lift jets of STOVL aircraft. The unsteady pressure loads on the lift plate, in the 160–165-dB range in the present case (loads as high as 175–180 dB have been measured for other conditions) are also significant and can lead to structural fatigue of nearby aircraft surfaces.

The high entrainment rates due to the presence of large-scale structures, such as those visible in Figs. 4a and 5a, lead to low pressures on the lift plate surface resulting in a suckdown force or lift loss. The lift loss variation with height can be seen in Fig. 9 for

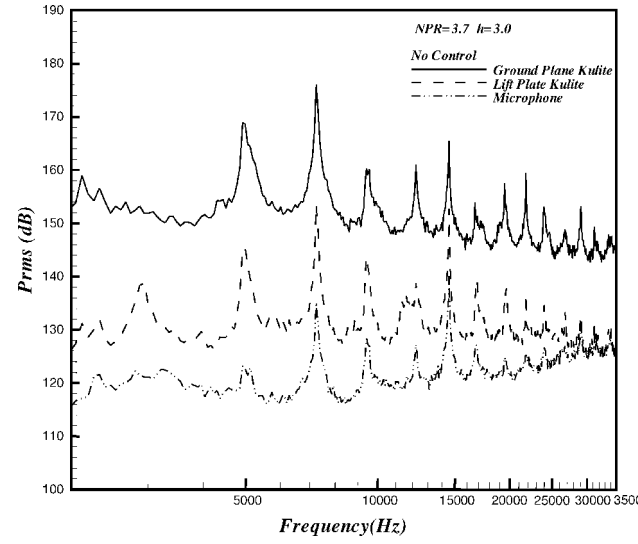

Fig. 6 Unsteady surface pressure and microphone spectra for NPR = 3.7 and $h/d = 3$.

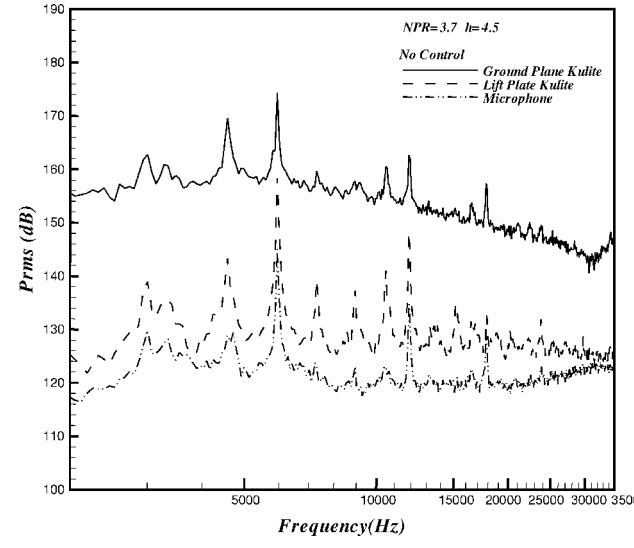

Fig. 7 Unsteady surface pressure and microphone spectra for NPR = 3.7 and $h/d = 4.5$.

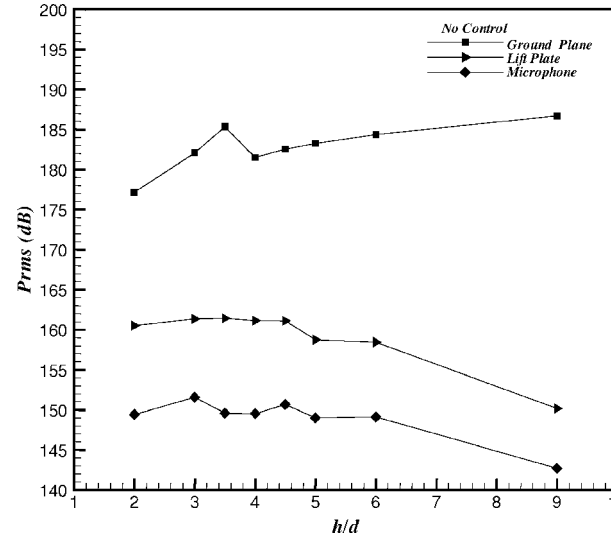

Fig. 8 Fluctuating pressure intensities for NPR = 3.7 and $h/d = 3.5$.

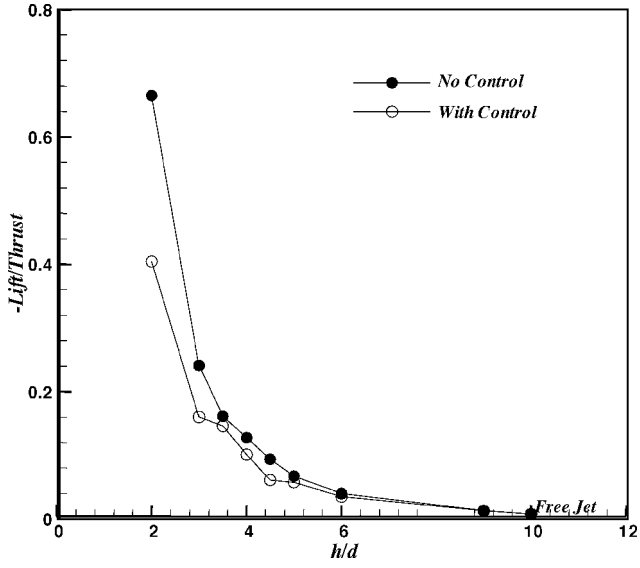

Fig. 9 Lift loss variation with ground plane distance, with and without control; NPR = 3.7.

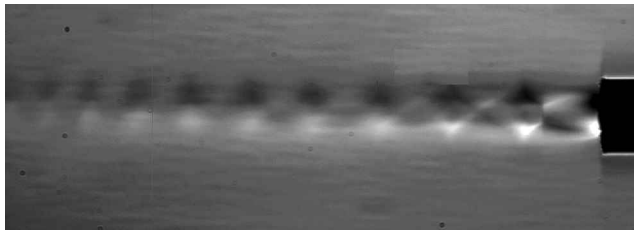

Fig. 10 Schlieren image of a supersonic microjet issuing from a 400-μm nozzle, $P_0 \sim 110$ psia.

the present case. Figure 9 shows the lift loss behavior with (open symbols) and without (filled symbols) microjet control, where the negative lift force has been normalized by the primary jet thrust. Figure 9 illustrates the dramatic lift loss for the uncontrolled case, as high 60% or more for small heights, which can occur due to jet impingement. Figure 9 also shows that, at least in terms of lift loss, ground effect become negligible for $h/d > 9$.

B. Impinging Jet with Microjet Control

In light of the detrimental effects of the feedback loop, an attempt to disrupt this feedback was made with the hope of alleviating some of these undesirable properties. In this study, flow control was applied by simply activating the supersonic microjets placed at the nozzle exit. It was anticipated that the penetration of the microjets into the primary jet shear layer at the nozzle exit would sufficiently modify the shear layer properties, including perhaps its stability characteristics, to disrupt this loop.

Figure 10 shows a representative schlieren image of one of the 400-μm microjets used to control the feedback loop. The microjet is operating at a pressure of approximately 100 psia, and the flow is clearly supersonic as demonstrated by the characteristic periodic shock-cell structure usually observed in much larger supersonic jets. From the presence of the shock cells, the supersonic core of the jet appears to extend at least 10–12 jet diameters downstream of the nozzle exit. A more detailed description of the supersonic microjets, their behavior, and the technique used for visualization may be found in Ref. 23. Given the high momentum associated with the supersonic microjets and the large supersonic core length, it is anticipated that they will serve as effective actuators capable of penetrating the primary jet shear layer and modifying its properties. Before discussing the results of microjet flow control, note that no attempt was made in the present study to modulate or manipulate the microjets actively in response to the local flow conditions. The results presented here only compare the relevant properties with and without the microjets.

A comparison of the instantaneous shadowgraphs without control (Fig. 4a) to that with control (Fig. 4b) shows the dramatic effect of activating the microjets. First, the strong acoustic waves present for the uncontrolled case have been eliminated when the microjets are activated. Furthermore, the large-scale shear layer structures readily visible in Figs. 4a and 5a have also been significantly reduced, if not entirely eliminated, in Figs. 4b and 5b. As anticipated, the elimination of the large-scale structures is accompanied by a reduction in the jet spreading rate and a narrowing of the jet column, as seen in Fig. 5b. Also visible in Fig. 5b are the streaks generated by the supersonic microjets. Such streaks are very similar to those generated by tabs[17,18] and tape elements on the nozzle surface[24]; they have been used as indication of the presence of substantial streamwise vorticity. Note that the presence of such tabs and the concomitant generation of streamwise vorticity have led to a suppression of screech tones[17,25]; this aspect will be very briefly discussed later in this paper.

Given the striking effect of the microjets observed in the shadowgraphs, one expects the unsteady flow properties to be similarly influenced. This is indeed the case as seen in the near-field narrowband frequency spectra for $h/d = 4.5$ in Fig. 11. Figures 11a and 11b show the ground and lift plate unsteady pressures, respectively, whereas Fig. 11c shows the near-field microphone spectrum. When the control data (solid lines) are compared to the uncontrolled case (broken lines), one observes that the distinct tones present in the uncontrolled impinging jet are either eliminated or significantly diminished by the activation of microjets. In addition, and perhaps more significantly, the attenuation in the discrete tones is accompanied by a broadband reduction in the spectral amplitudes. This broadband reduction is observed for all three plots (Figs. 11a–11c) due to lower acoustic and hydrodynamic fluctuations, which suggests a global decline in the unsteady behavior of this flow.

The overall unsteady pressure levels P_{rms} on the lift plate at different heights and the influence of microjet control at each location are shown in Fig. 12. Note that the error bars shown at selected data points are representative of the errors over the range of conditions shown here. Figure 12 plainly shows that the fluctuating loads on the lift plate are reduced with the activation of microjet control. However, the magnitude of reduction is strongly dependent on h/d, the ground plane distance. Whereas a very substantial reduction of more than 10 dB is achieved at $h/d = 4.5$, the unsteady load is only reduced by 2 dB or so at $h/d = 3.5$. The nonuniform reductions illustrate that the control technique is not equally efficient at all heights, presumably because it does not track changes in the feedback loop due to a variation in h/d. The reductions in the overall unsteady pressure and acoustic intensities on the lift and ground planes and for the near-field microphone measurements are summarized in Fig. 13. Similar to the behavior observed in Fig. 12, the reductions in flow unsteadiness due to microjet control are strongly dependent on the ground plane height. However, notably, the overall trends for all three measurements are very similar with the greatest reductions achieved at $h/d = 3$ and 4.5. Once again, the nonmonotonic influence of control suggests that efficient control of this flow requires an adaptive control approach where the microjets can be actively manipulated to provide optimal control at all heights.

As observed earlier, the unsteady behavior of the impinging jet, including the hydrodynamic and acoustic loads generated by this flowfield, is highly sensitive to the local boundary conditions. Hence, these properties are not only a function of the operating conditions, such as h/d or NPR as shown in Figs. 8 and 13, but can also change somewhat when an experiment is repeated under the same conditions. Consequently, the efficacy of the control technique, for example, its variation with h/d (Fig. 13), can also vary between experiments, even if there are very minor changes in the flow conditions. However, on repeating these experiments a number of times, our results consistently show that although minor shifts in the performance (with h/d) can occur due to minor changes in the flow properties, the changes are global in nature, that is, they occur at all measurement locations, the lift plate, ground plane, and the

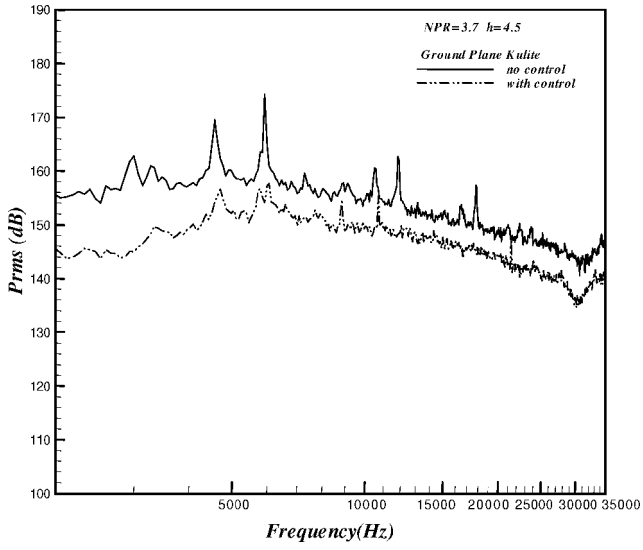

a) Ground plane

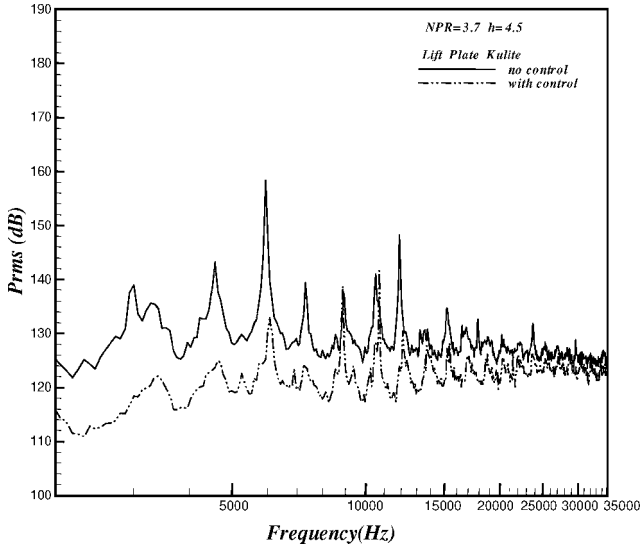

b) Lift plate

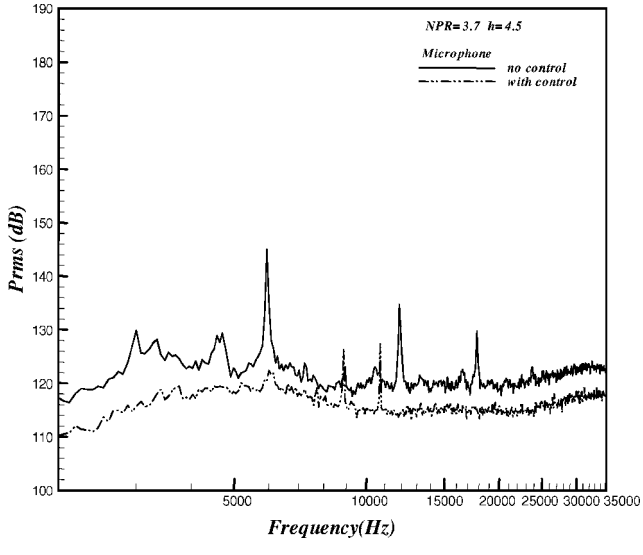

c) Microphone

Fig. 11 Unsteady pressure and microphone spectra with and without control; NPR = 3.7, h/d = 4.5.

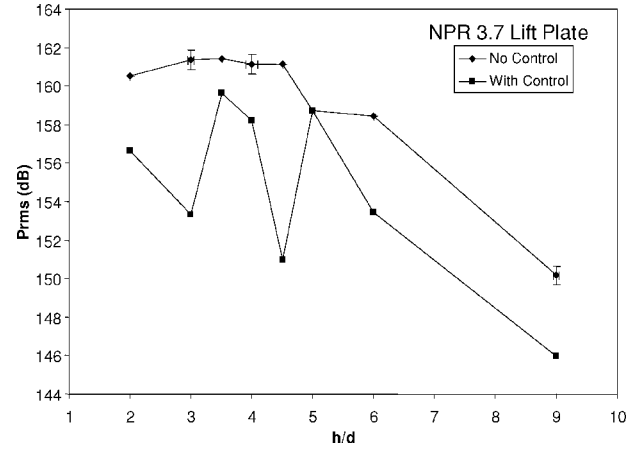

Fig. 12 Fluctuating pressure intensities on the lift plate, with and without control; NPR = 3.7.

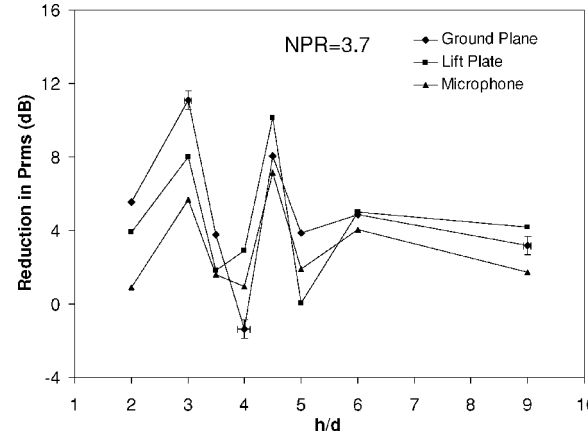

Fig. 13 Reduction in fluctuating pressure intensities; NPR = 3.7.

near-field acoustics. The error bars shown on Fig. 13 roughly span the extent of such variations observed for the present study. This dependence once again emphasizes the need for adaptive control. (See Ref. 21 for further discussion.)

Finally, we present the effect of microjets on the lift loss behavior of this flow. Because the loss in lift is due to the low pressures created on the underside of the airframe, the lift plate in this study, due to flow entrainment by the large-scale structure, it is logical to assume that elimination or reduction of these structures should also result in a reduction in lift loss. Measurements of the mean static pressures on the lift plate surface show that the activation of supersonic microjets leads to an increase in the surface pressures, that is, to lower vacuum/suction pressures on the lower surfaces of the airframe. This reduction in the vacuum pressures on the lift plate translates to a reduction in lift loss as seen in Fig. 9. A comparison of the open symbols (with control) to filled symbols (no control) in Fig. 9 shows that the activation of microjets leads to a significant reduction in lift loss. The maximum lift loss recovery occurs for small heights, for example, the lift loss is reduced by more than 40% at $h/d = 2$, with the influence becoming less significant for larger heights. This behavior is expected and desirable because the largest losses in lift also occur for small separations. Figuer 14 is a summary of the lift loss reduction variation with h/d. The reduction in lift loss in Fig. 14 behaves in a manner similar to the trends observed in Fig. 13 on the influence of microjets on unsteady pressures and noise; Fig. 14 confirms that control effectiveness varies nonuniformly with h/d. Moreover, a comparison of Fig. 14 to the reduction in P_{rms} on the lift plate shown in Fig. 13 shows the similarity between the two plots where the local minima and maxima in lift loss recovery occur at roughly the same heights as the local minima and maxima in the reduction in the fluctuating pressures (Fig. 13). This again

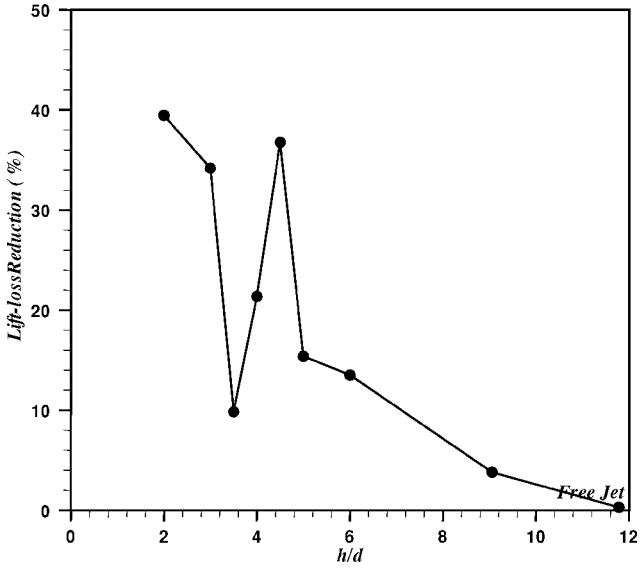

Fig. 14 Lift loss recovery variation as a function of ground plane distance.

suggests a strong correlation between the strength of the acoustic waves impinging on the lift plate (Fig. 4a), which are expected to be the primary source of unsteady loads on the lift plate, and the large-scale structures, which lead to lift loss. Given the global nature of the unsteady properties, such a connection is expected.

The nonuniform behavior in the reductions in lift loss, fluctuating pressures, and noise, reinforces the notion that an adaptive control strategy is necessary to achieve optimal performance at all operating conditions. Nevertheless, even without adaptive control, microjets are a rather effective control tool at most heights where they result in notable reductions in unsteady loads in the range of 4–10 dB and a lift loss recovery of 20% or higher for small h/d.

C. Physical Mechanisms Behind Microjet Control

Before concluding, we very briefly discuss the possible physical mechanisms that may be responsible for the efficient disruption of the feedback loop by microjets. As mentioned earlier, there are many potential ways by which one can disrupt the feedback loop. The interception of the upstream propagating acoustic waves before reaching the shear layer at the nozzles exit was one of the possible ways the feedback may be interrupted. However, we believe that, although the microjets may provide some shielding of the shear layer at the nozzle exit, given the extremely small size of the microjets, the shielding effect will not be significant. The disruption of the spatial coherence of the interaction between the acoustic waves and the shear layer at the nozzle exit is another such possible mechanism. Our results suggest that the spatial extent of the disruption by the microjets does play some role in reducing the efficacy of the feedback mechanism, in that when the number of microjets were reduced beyond a certain threshold, the feedback loop was minimally disrupted. However, reducing the number of microjets also reduces the amount of streamwise vorticity introduced into the primary jet, which as discussed next, may be the significant mechanism behind the success of this technique. Hence, at present, it is difficult to quantify the exact extent to which the disruption of the spatial coherence plays a role except to say that it does play some role in attenuation of the feedback.

We believe that the most significant reason for the weakening of the feedback is due to the redirection of some of the significant azimuthal vorticity, manifested as large-scale structures in the shear layer, into streamwise vorticity as a result of microjet injection. This hypothesis is supported by preliminary measurements of the streamwise vorticity in the shear layer, which revealed that the activation of microjets leads to the generation of significant streamwise vorticity. The streamwise vorticity, manifested in the form of pairs of counter-rotating vortices corresponding to the microjet locations, is generated at the expense of the azimuthal vorticity, thereby weakening the large-scale structures and, hence, the feedback loop. To shed some light on the role of microjets relative to more traditional approaches such as the use of tabs, a limited number of experiments were conducted using 16 microtabs instead of microjets. These microtabs were made by using stainless wires of the same diameter as the microjets, placed at the nozzle exit, protruding five (microjet) diameters into the jet shear layer. These microtabs produced almost no reduction for the ideally expanded impinging jet, suggesting that the flow physics behind the present technique is different.

Although many questions remain unanswered at present, it is clear from the results presented here that microjet control is a very effective and potentially useful control approach for impinging jets. It is also likely that more than one mechanism, for example, redirection of the azimuthal vorticity, disruption of the spatial coherence of the interaction, among others, may play a role in the physics behind this method. Presently, we are conducting experiments that are more detailed to better understand some of these physical mechanisms and their relative influence.

IV. Conclusions

Previous investigators have unequivocally established the intimate connection between the fluid dynamic and acoustic properties of the impinging jet flowfield, an interaction that occurs through a feedback loop. The occurrence of this feedback loop was also hypothesized to be responsible for a number of performance diminishing effects for STOVL aircraft.[10]

The objective of this research program is to develop a practical control strategy to enhance the STOVL aircraft performance under realistic operating conditions by taking advantage of our understanding of the aeroacoustic properties of this flow. In this paper, we explored a novel control technique utilizing supersonic microjets to disrupt the feedback mechanism in supersonic impinging jet flows. The disruption of this feedback mechanism through this control technique resulted in significant performance gains relative to the uncontrolled case. Lift loss was substantially reduced, by as much as 40%, accompanied by a 10–11-dB reduction in the fluctuating pressure loads on the lift and ground surfaces for certain conditions. Similarly, the overall noise levels were substantially reduced and the discrete, high-amplitude impinging tones ubiquitous in such flows were either eliminated or significantly attenuated.

However, the performance enhancements due to microjet control were not uniform over the entire parametric space. We believe this is because the microjets are presently used in a passive mode. Because of the dynamic nature of this flow, the properties of the flow–acoustic interactions change with operating conditions. Hence, an optimal control technique must be able to adapt to these changes. We are presently exploring ways of actively manipulating the supersonic microjets to respond to the changing environment. We are also developing on-demand control methods using integrated sensors and supersonic microjet actuators. In future studies, we expect to implement these control techniques in more realistic planform geometries utilizing single and dual supersonic impinging jets.

Acknowledgments

Our research program on short takeoff and vertical landing aircraft jet-induced effects is supported by NASA Ames Research Center (Technical Monitor, Doug Wardwell), the Air Force Office of Scientific Research (Technical Monitor, currently John Schmisseur, previously, Steven Walker), and The Boeing Corporation. We also thank the students and staff at the Fluid Mechanics Research Laboratory for their help in conducting these experiments, especially K. Phalnikar for characterizing the supersonic microjets and H. Lou for editing some of the figures.

References

[1]Elavarasan, R., Ventkatakrishnan, L., Krothapalli, A., and Lourenco, L., "Supersonic Twin Impinging Jets," AIAA Paper 2000-0812, Jan. 2000.

[2]Powell, A., "The Sound-Producing Oscillations of Round Underexpanded Jets Impinging on Normal Plates," *Journal of the Acoustical Society of America*, Vol. 83, No. 2, 1988, pp. 515–533.

[3]Neuwerth, G., "Acoustic Feedback of a Subsonic and Supersonic Free Jet Which Impinges on an Obstacle," NASA TT F-15719, May 1974.

[4]Tam, C. K. W., and Ahuja, K. K., "Theoretical Model of Discrete Tone Generation by Impinging Jets," *Journal of Fluid Mechanics*, Vol. 214, 1990, pp. 67–87.

[5]Powell, A., "On the Mechanism of Choked Jet Noise," *Proceedings of the Physical Society, London*, Sec. B66, 1953, pp. 1039–1057.

[6]Powell, A., "On Edge Tones and Associated Phenomena," *Acoustica*, Vol. 3, 1953, pp. 233–243.

[7]Donaldson, C. DuP., and Snedeker, R. S., "A Study of Free Jet Impingement. Part 1. Mean Properties of Free and Impinging Jets," *Journal of Fluid Mechanics*, Vol. 45, 1971, 281–319.

[8]Carling, J. C., and Hunt, B. L., "The Near Wall Jet of a Normally Impinging, Uniform, Axisymmetric, Supersonic Jet," *Journal of Fluid Mechanics*, Vol. 66, Oct. 1974, 159–176.

[9]Lamont, P. J., and Hunt, B. L., "The Impingement of Underexpanded Axisymmetric Jets on Perpendicular and Inclined Flat Plates," *Journal of Fluid Mechanics*, Vol. 100, 1980, pp. 471–511.

[10]Krothapalli, A., Rajakuperan, E., Alvi, F. S., and Lourenco, L., "Flow Field and Noise Characteristics of a Supersonic Impinging Jet," *Journal of Fluid Mechanics*, Vol. 392, Aug. 1999, pp. 155–181.

[11]Alvi, F. S., and Iyer, K. G., "Mean and Unsteady Flowfield Properties of Supersonic Impinging Jets with Lift Plates," AIAA Paper 99-1829, May 1999.

[12]Karamcheti, K., Bauer, A. B., Shields, W. L., Stegen, G. R., and Woolley, J. P., "Some Features of an Edge Tone Flow Field," NASA SP 207, 1969, pp. 275–304.

[13]Elavarasan, R., Krothapalli, A., Venkatakrishnan, L., and Lourenco, L., "Suppression of Self-Sustained Oscillations in a Supersonic Impinging Jet," *AIAA Journal*, Vol. 39, No. 12, 2001, pp. 2366–2373.

[14]Elavarasan R., Venkatakrishnan, L., Krothapalli, A., and Lourenco, L., "A PIV Study of a Supersonic Impinging Jet," *Journal of Visualization*, Vol. 2, No. 3/4, 2000, pp. 213–222.

[15]Glass, D. R., "Effect of Acoustic Feedback on the Spread and Decay of Supersonic Jets," *AIAA Journal*, Vol. 6, No. 6, 1968, pp. 1890–1897.

[16]Poldervaart, L. J., Wijnands, A. P. J., vanMoll, L. H. A. M., and vanVoorthuisen, E. J., "Modes of Vibration," *Journal of Fluid Mechanics*, Vol. 78, 1976, pp. 859–862.

[17]Samimy, M., Zaman, K. B. M. Q., and Reeder, M. F., "Effect of Tabs on the Flow and Noise Field of an Axisymmetric Jets," *AIAA Journal*, Vol. 31, No. 4, 1993, pp. 609–619.

[18]Zaman, K. B. M. Q., Reeder, M. F., and Samimy, M., "Control of an Axisymmetric Jet Using Vortex Generators," *Physics of Fluids*, Vol. 6, No. 2, 1994, pp. 778–793.

[19]Sheplak, M., and Spina, E. F., "Control of High-Speed Impinging-Jet Resonance," *AIAA Journal*, Vol. 32, No. 8, 1994, pp. 1583–1588.

[20]Shih, C., Alvi, F. S., and Washington, D., "Effects of Counterflow on the Aeroacoustic Properties of a Supersonic Jet," *Journal of Aircraft*, Vol. 36, No. 2, 1999, pp. 451–457.

[21]Lou, H., Alvi, F. S., Shih, C., Choi, J., and Annaswamy, A., "Active Control of Supersonic Impinging Jets: Flowfield Properties and Closed-Loop Strategies," AIAA Paper 2002-2728, June 2002.

[22]Wardwell, D. A., Hange, C., Kuhn, R. E., and Stewart, V. R., "Jet-Induced Ground Effects on a Parametric Flat-Plate Model in Hover," NASA TM 104001, 1993.

[23]Phalnikar, K., Alvi, F. S., and Shih, C., "Behavior of Free and Impinging Supersonic Microjets," AIAA Paper 2001-3047, June 2001.

[24]Krothapalli, A., Strykowski, P. J., and King, C. J., "Origin of Streamwise Vortices in Supersonic Jets," *AIAA Journal*, Vol. 36, No. 5, 1998, pp. 869–872.

[25]Tanna, H. K. "An Experimental Study of Jet Noise, Part II, Shock Associated Noise," *Journal of Sound and Vibration*, Vol. 50, No. 3, 1977, pp. 429–444.

A. Plotkin
Associate Editor